



UNIVERSITY OF LEEDS

This is a repository copy of *Electro-coalescence of water drops in oils under pulsatile electric fields*.

White Rose Research Online URL for this paper:  
<http://eprints.whiterose.ac.uk/81431/>

Version: Accepted Version

---

**Article:**

Mousavi, SH, Ghadiri, M and Buckley, M (2014) Electro-coalescence of water drops in oils under pulsatile electric fields. *Chemical Engineering Science*, 120. 130 - 142. ISSN 0009-2509

<https://doi.org/10.1016/j.ces.2014.08.055>

---

**Reuse**

Unless indicated otherwise, fulltext items are protected by copyright with all rights reserved. The copyright exception in section 29 of the Copyright, Designs and Patents Act 1988 allows the making of a single copy solely for the purpose of non-commercial research or private study within the limits of fair dealing. The publisher or other rights-holder may allow further reproduction and re-use of this version - refer to the White Rose Research Online record for this item. Where records identify the publisher as the copyright holder, users can verify any specific terms of use on the publisher's website.

**Takedown**

If you consider content in White Rose Research Online to be in breach of UK law, please notify us by emailing [eprints@whiterose.ac.uk](mailto:eprints@whiterose.ac.uk) including the URL of the record and the reason for the withdrawal request.



[eprints@whiterose.ac.uk](mailto:eprints@whiterose.ac.uk)  
<https://eprints.whiterose.ac.uk/>

# Effect of Pulsatile Electric Fields on Electrocoalescence of Water Drops in Oils

S. H. Mousavi<sup>1,2</sup>, M. Ghadiri<sup>1\*</sup>, M. Shariaty-Niassar<sup>2</sup>, M. Buckley<sup>1</sup>

<sup>1</sup>Institute of Particle Science and Engineering, University of Leeds, LS2 9JT, United Kingdom

<sup>2</sup>Faculty of Caspian, College of Engineering, University of Tehran, 11365-4563 Tehran, Iran

\* Corresponding author's email: m.ghadiri@leeds.ac.uk

## Abstract

For the separation of dispersed water drops from oils an electric field may be used to enhance their coalescence. However, this process could cause some undesirable phenomena such as secondary droplets formation, reducing the separation efficiency. Here the effect of pulsatile electric fields (PEF) on the secondary droplets formation has been investigated. In the presence of a very low frequency PEF or DC electric field three distinct drop-drop and drop-interface interaction patterns are observed: complete coalescence, partial coalescence and rebound without coalescence. The first is the ideal pattern not leaving any secondary droplets. It has previously been shown that an increase in the electric field strength and/or a decrease in the interfacial tension result in non-ideal patterns in drop-interface coalescence. The application of PEF shifts the coalescence pattern from a non-ideal to an ideal one in both drop-drop and drop-interface coalescences. Three waveform types, i.e. square, sinusoidal and sawtooth waves have been applied to the coalescence process. It is shown that the sawtooth waveform is the most effective in reducing the secondary droplets formation in drop-interface coalescence, followed closely by the sinusoidal one. The observation of videos sequences suggests that a threshold frequency exists above which a non-ideal pattern switches to an ideal one. For drop-drop coalescence this threshold frequency depends on the PEF amplitude and the size of primary drop pairs, as for bigger primary drop pairs and larger amplitudes of PEF the threshold frequency would be higher. When using pulsatile electric fields higher field strengths can be applied for systems having a high water content without causing field breakdown, as compared to constant DC field. This is useful in optimizing the electro-coalescence process.

**Keywords:** electro-coalescence, secondary droplets, pulsatile electric field, drop-drop coalescence, drop-interface coalescence, coalescence patterns, surfactant, threshold frequency.

## 1. Introduction

Dispersed water drops in organic liquids, such as water-in-crude oil emulsions, are commonly encountered in the oil, chemical and biochemical industries [1-3]. The formation of water-in-crude oil emulsion during oil production is undesirable from both a process and product quality point of view. Natural coalescence of drops in such emulsion is constrained because of a thin film of oil between drops not allowing their spontaneous coalescence, and consequently water-in-crude oil emulsions, despite being thermodynamically unstable, can be kinetically very stable for long periods of time [4, 5]. The emulsion stability can be due to the presence of naturally occurring surfactants in the crude oil, such as asphaltenes, resins, waxes, and naphthenic acids [6-8]. Asphaltenes and resins are the heaviest and the most polar fraction of the

crude oil and are believed to be the major components responsible for emulsion stabilization [9-11]. When the asphaltenes accumulate at water-in-crude oil interfaces they tend to form a rigid film surrounding the water drop, thereby preventing them to coalesce during drop-drop collisions [6]. This constraint will be increasingly crucial in future since the amount of water produced will be increasing in mature fields. These emulsions have to be separated into their constituent phases before the subsequent operations, due to process requirements, environmental regulations and customer specifications, as in the case of crude oil industry [3].

Water droplets can be removed from a continuous oil phase by several methods [12], such as chemical demulsifiers [13, 14], gravity or centrifugal separation [15, 16], pH adjustment and heating treatment [12, 17] and membrane filtration separation [12, 15]. However, nowadays one of the most effective and utilized method from viewpoint of energy efficiency is electrostatic demulsification. The combination of high energy efficiency, since it permits a reduction of the use of heat, and also the fact that it avoids the use of chemical demulsifiers makes this technique environmentally friendly [18-20].

The utilization of electrical methods for dehydrating crude oil emulsions is not new and has been well reviewed [3, 21-25]. In the petroleum industry, the first work on electro-coalescence dates from the work of Cottrell in applying external electric fields to crude-oil emulsions [26, 27]. Electro-coalescence is a process to assist approach, contact and finally coalescence of water droplets in oils with a low dielectric permittivity in order to increase their size, thus accelerating their settling velocity and reducing their separation time. The electrostatic effects arise from differences in properties of oil and water, where water has dielectric permittivity and conductivity values much higher than those of the oil, leading to polarization effects in water drops [10]. The amount of dispersed aqueous phase is a key feature to choose the type of electric field. Historically the alternative current (AC) electric field is the oldest and commonest configuration used extensively in crude oil emulsion treatment, as it can tolerate high water contents [3]. In contrast, the direct current (DC) electric field has been less common in the past and has been used more in the treatment of refinery emulsions with low water content in order to reduce electrolytic corrosion. Generally, the presence of an electric field promotes contacts between drops, enhancing drop-drop and drop-interface coalescence [3, 23, 28]. Hence, research has been carried out on the application of various types of electric fields in the electro-coalescence at a micro-scale level [22, 29-36].

In 1986, Bailes [37] introduced the use of pulsed DC electric fields with insulated electrodes for the treatment of high aqueous content emulsions [23, 38]. Drelich et al. [39] studied emulsions containing 0.08-0.2 wt% dispersed water with droplet diameters below 20  $\mu\text{m}$  in a continuous flow electrostatic coalescer and reported a separation efficiency of about 63%, when the pulse electric field strength was 140 kV/m for three frequencies 5, 10 and 15 Hz. According to their experiments, the frequency of pulsed DC electric field exerted no significant influence on the demulsification yield in the range studied (5 to 25 Hz). Nevertheless, a maximum in separation efficiency was observed for pulsation frequencies between 8 Hz and 11 Hz. Less et al. [40] considered the influence of several operational variables including shear rate, temperature, emulsion water content, electric field strength, and application time on the electro-coalescence of water-in-oil emulsions under the influence of an AC electric field and showed all play a prominent role in the process. They reported the electric field strength is beneficial only up to a limiting value, above which the probability of droplet break up increases. Bailes et al. [41, 42] reported that a better efficiency of electro-coalescence can be gained by pulsed DC electric fields in comparison with constant DC or AC fields.

Bailes and Dowling [43] established that pulsed unidirectional voltages applied to electrodes insulated from the liquids is an efficient means of promoting phase disengagement particularly for dispersions with a high conducting phase content. They also showed that the rate of coalescence was not only a function of pulse amplitude but also of its shape, mark to space ratio and frequency; all of these parameters having physical optimum values. Lesaint et al. [19] studied the efficiency of removal of water drops with AC electric fields using model oil emulsions and indicated that not only the application time, waveform, strength and frequency of the applied electric field, but also the temperature all play a notable role in the process.

Zhang et al. [44] investigated the influence of several operational variables on the electrostatic separation of water-in-oil emulsions subjected to a high-frequency pulsed DC electric field (higher than 1 kHz) using conductivity technique. They reported that the dehydration efficiency (DE) for a given inter-electrode distance increases with decreasing frequency. Moreover, they found that pulse duration also affected the dehydration ability. At a given inter-electrode distance and pulse interval, DE increased with increasing pulse duration. Also Zhang et al. [45] investigated the dehydration efficiency of pulsed DC electric field as a function of frequency. Their results showed that at an appropriate range of frequencies, the dehydration efficiency of the pulsed DC electric field could be improved significantly. Eow and Ghadiri [22] observed when a pulsed electric field was applied to a drop, it vibrated with the same frequency as the applied pulse frequency until a limit, above which the drop vibrated at a lower frequency than the applied pulse frequency. The limit depended on the continuous liquid phase. In addition, they showed above this limit, the drop had smaller amplitude of vibration.

Midtgård [46] presented a mathematical analysis of the electric field and interfacial free charge experienced by the emulsion in an electrostatic coalescer that was subjected to a pulsed DC voltage. He presented a novel analysis of the system giving valuable physical insight and showed that there must be a limited range of frequencies that are effective in a pulsed DC scheme.

Mousavichoubeh et al. [33, 34] studied the partial coalescence process and established that the strength of a DC field and interfacial tension affected the tendency of secondary droplet formation. They showed that the volume fraction of secondary droplets could be described by coupling the Weber number with the Ohnesorge number. Two competing processes of necking and pumping were distinguished as a result of electrostatic and surface tension forces, respectively, which determined whether secondary droplets formed or not. The necking process attempts to separate the secondary droplets and the pumping process drains the content of drop into the homophase under interface, leading to a complete coalescence. The droplet deformation and necking due to the electric field is described by the Weber number ( $We = 2r\epsilon_{oil}\epsilon_0E_0^2/\sigma$ , where  $r$  is drop radius,  $\epsilon_{oil}$  is dielectric constant of continuous phase,  $\epsilon_0$  is permittivity of vacuum,  $E_0$  is background electric field strength and  $\sigma$  is interfacial tension), whilst the pumping of water drop content into the homophase under interface in the process of coalescence is described by the Ohnesorge number ( $Oh = \mu/(\rho r\sigma)^{0.5}$ , where  $\mu$  and  $\rho$  are viscosity and density of drop phase). Mousavichoubeh et al. [33, 34] showed that the product of these two dimensionless groups  $WO = We \times Oh$  describes well the volume fraction of secondary droplets that are formed.  $WO$  Number represents the ratio of the electrical stress energy that causes necking over the energy required for pumping the viscous fluid out of the droplets. For a wide

range of interfacial tensions, brought about by the use of non-ionic and anionic surfactants and electric field strengths, a good unification of data was reported.

In agreement with Mousavichoubeh et al. [33, 34], Hamlin et al. [47] reported that the extent of coalescence between dissimilarly sized water drops in oil can be tuned from complete coalescence at low DC electric field strengths to complete noncoalescence at high field strengths. They investigated the effect of conductivity on the coalescence of oppositely charged drops in the presence of a DC electric field and showed the charge transfer between primary and daughter droplets and the size of daughter droplets are unexpectedly independent of the ionic conductivity. To make prediction about daughter droplets formation, they presented evidence suggesting the charge transfer is strongly influenced by convection associated with the capillary-driven penetration of a vortex into the larger drop rather than conductivity.

In this paper we report our investigations on the effect of pulsed electric fields on suppressing the secondary droplets formation for both drop-drop and drop-interface coalescence processes.

## 2. Experimental set-up and procedures

The experimental cell is the same as used in our previous work [33, 34]. The cell is made of Perspex to facilitate visualisation of the coalescence phenomenon. The electrodes are polished brass plates with dimensions of 90 mm  $\times$  25 mm. The high voltage electrode is attached to the upper part of the cell, which is movable to set the distance to create the required electric field strength. There is a small hole through the mid-point of the upper part of the cell and brass plate to allow a hypodermic needle to pass through it. The needle, attached to a syringe (Hamilton micro-liter syringe) is used to introduce small aqueous droplets in the cell on the interface or falling on the second primary drop in the case of drop-drop coalescence. The needle is grounded in order to ensure that uncharged drops are produced. The high voltage electrode is connected to a positive polarity high voltage direct current power amplifier (TREK 20/20C) and the bottom electrode is grounded. A high-speed digital video camera (Photron FASTCAM SA5), equipped with a micro lens (NAVITAR 12 $\times$  Zoom Lens) was used to observe the phenomena within the cell and it was focused either on the centre of the water-oil interface or on the area limited to coalescing drop pairs. This camera was used with a framing rate of 20000 fps. In drop-drop experiments, the grounded electrode was coated with a thin layer of Perspex so that charging of the primary drops settling on the bottom of the cell was avoided. The strength of the electric field can be affected as a result of Perspex insulator stuck on the grounded electrode [39]. Nevertheless, the decrease of the electric field strength is less than 1%, since the insulator is 1 mm in thickness in comparison with the large inter-electrodes distance.

In this work the electro-coalescence cell is used in two ways: either the cell is entirely filled with a dielectric oil to conduct the drop-drop coalescence experiments or the bottom half of the cell is filled with water and the top half with the oil to form an interface of two phases and proceed with the drop-interface coalescence experiments. In the experiments reported here sunflower oil was used. A halogen cold lamp (Dedolight DLHM4-300) with four flexible fibre optic heads was used for lighting; the intensity of the lighting could be accurately adjusted to

facilitate focusing. De-ionized water either on its own or containing a surfactant was used as the dispersed phase, while the continuous phase was pure sunflower oil (obtained from Morrisons Ltd, UK). The properties of the liquids used in this research and interfacial tension values for solutions are given in Tables 1 and 2, respectively, and are exactly the same as those used in our previous work [36], where further details of the experimental procedure are given.

Table 1. The properties of the liquid used in the experiments [36]

Liquids	Conductivity ( $\mu\text{Sm}^{-1}$ ) ( $\pm 5\%$ )	Viscosity (mPa.s) ( $\pm 5\%$ )	Density ( $\text{kgm}^{-3}$ ) ( $\pm 5\%$ )	Dielectric constant
De-ionised water	5.49	1.00	1000	80
Sunflower oil	$7.62 \times 10^{-5}$	46.5	922	4.9
De-ionised water including 1g/l SDS	242	$\approx 1.00$	$\approx 1000$	$\approx 80$

Table 2. Interfacial tensions [36]

Liquids	Interfacial tension <sup>a</sup> ( $\text{mNm}^{-1}$ )
De-ionised water-Sunflower oil	25
1 g/l SDS in dispersed phase- pure Sunflower oil	10

<sup>a</sup> Interfacial tension measured at 21 °C and 1 atm.

Water droplets of different sizes were produced using hypodermic needles in droplet diameter range between 576  $\mu\text{m}$  to 1196  $\mu\text{m}$ . The diameter of the droplets was measured by the use of Image-Pro and PFV (Photron Fastcam Viewer ver. 320) software. The standard deviations were in the range from 1-4  $\mu\text{m}$ . The diameter of the needle was measured by a microscope and was used for the in-situ calibration of the droplet size and measurements on the drop(s) plane. Three waveforms were used to consider the effect of waveform on the formation of secondary droplets. The fast charging capability of the high voltage unit ensured that the rise time was much less than the period of the wave (by one order of magnitude). The experiments were performed at  $22 \pm 1$  °C.

### 3. Results and discussion

#### 3.1. Drop-Interface coalescence

To investigate the effect of PEF on drop-interface coalescence, time sequences of coalescence of a drop with a diameter of  $984 \pm 2$   $\mu\text{m}$  under a square waveform PEF with an amplitude of 292 V/mm and pulse frequencies of 3, 40, and 110 Hz are shown in Figs 1, 2 and 3, respectively. In all these experiments the distance of the camera lense and drop plane was kept constant. Hence the size of the secondary droplets is truly comparable in three figures.

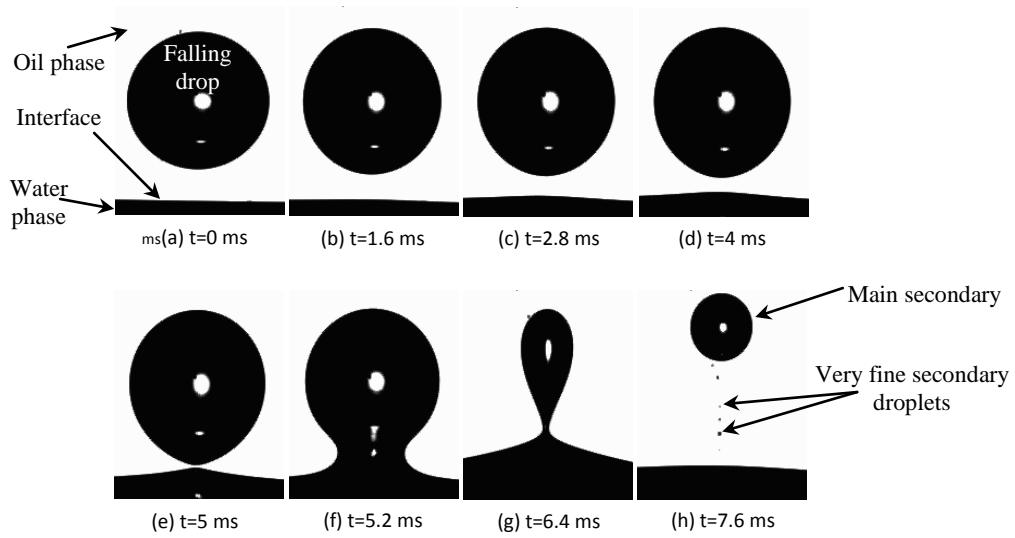


Fig. 1. Drop-interface coalescence of a drop with a diameter of  $984 \pm 2 \mu\text{m}$  under square waveform pulsed electric field with amplitude of  $292 \text{ V/mm}$  and frequency of  $3 \text{ Hz}$ .

As it is clearly seen in Figs 1(h), 2(p) and 3(r), by increasing the pulse frequency, the volume of the secondary droplets (mostly a main droplet and a tail following it which finally breaks into some very fine droplets) decreases, an undesirable trend in water-in-oil emulsions treatment.

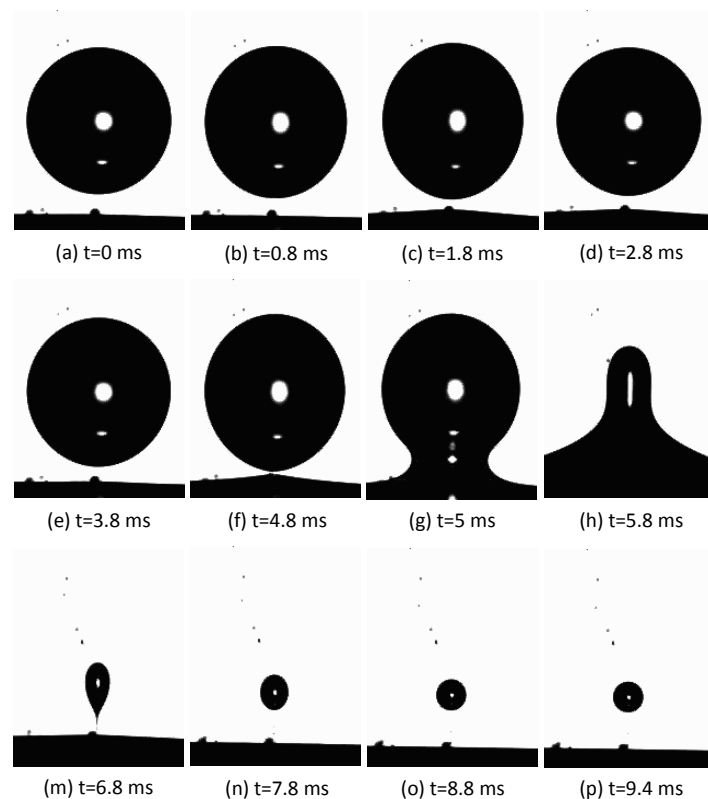


Fig. 2. Drop-interface coalescence of a drop with a diameter of  $984 \pm 2 \mu\text{m}$  under square waveform pulsed electric field with amplitude of 292 V/mm and pulse frequency of 40 Hz.

A similar behaviour is observed for the sinusoidal and sawtooth waveforms ([Supplementary movie #1](#)). To quantify the extent of secondary droplets formation and to show the suppressing effect of PEF, the volume ratio of secondary droplets over the initial drop was determined by image analysis and is given in Fig. 4 for frequencies up to 500 Hz.

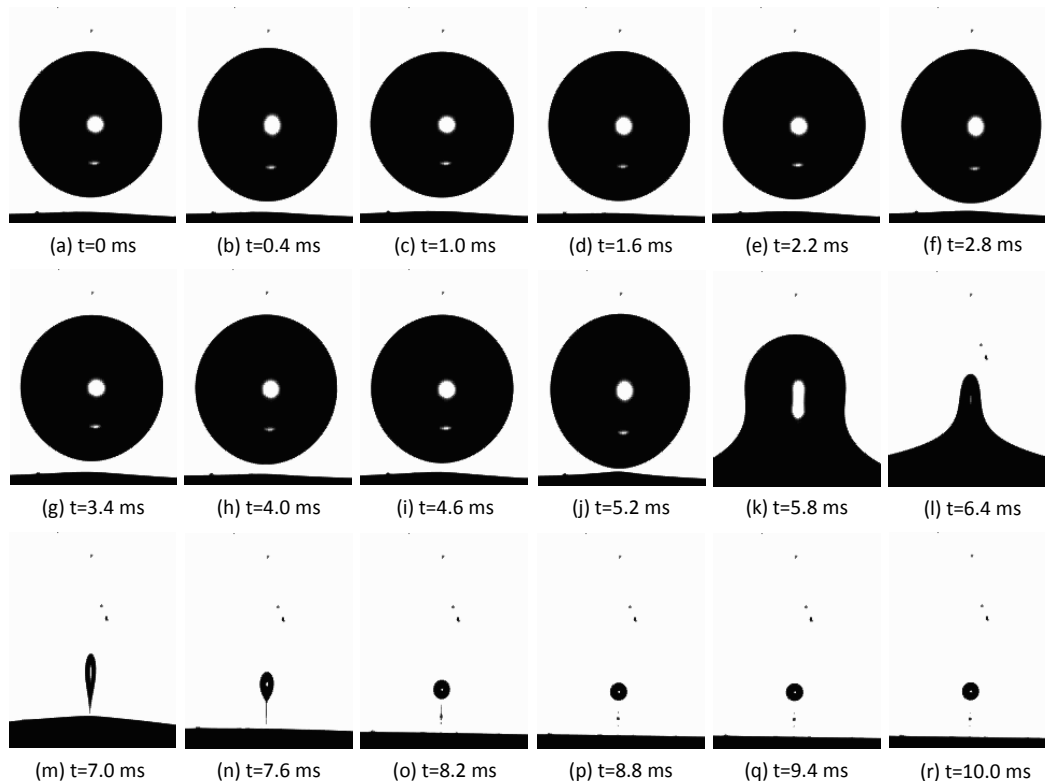


Fig. 3. Drop-interface coalescence of a drop with a diameter of  $984 \pm 2 \mu\text{m}$  under square waveform pulsed electric field with amplitude of 292 V/mm and pulse frequency of 110 Hz.

Initially the volume ratio decreases rapidly for all waveforms, but thereafter it gradually approaches an asymptotic value close to zero around 30 Hz for the sinusoidal and sawtooth wave forms, but for the square wave form the asymptotic approach is oscillatory and does not get to zero within the range tested.

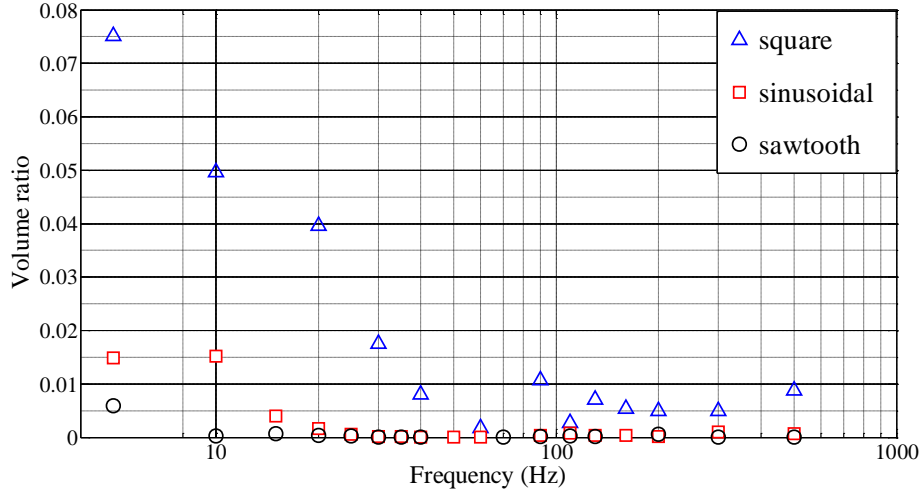


Fig. 4. Normalized volume of secondary droplets resulted from the application of a PEF with amplitude of 292 V/mm with different waveforms to a drop with diameter of  $984 \pm 2 \mu\text{m}$

The above observations can be interpreted by taking into account the constituent parts of a typical wave. An exaggerated schematic diagram of a typical wave is shown in Fig. 5, identifying four sections of the period,  $t_r$ ,  $t_{on}$ ,  $t_f$  and  $t_{off}$ . When a conductive drop is exposed to such a pulsed electric field, the drop starts elongating in the direction of the electric field and takes an elongated shape (ellipsoidal) during the on-time period and it starts to return to its unstressed form, i.e. spherical shape, in the fall time period, depending on the mechanical and electrical relaxation time constants. In all these stages the surface tension, inertia and viscous effects resist drop deformation, whilst the charge separation/polarisation acts in the opposite. However for very low frequencies the mechanical forces are smaller in comparison with the electrostatic force, which is responsible for drop deformation. This results in the oscillation frequency of drop following the field frequency. Increasing the pulse frequency makes the inertia effect grow; when the inertia forces become of the same order as the capillary and electrostatic force, the frequency of drop oscillation can no longer follow the field frequency. When the primary drop comes into contact with the interface at very low frequencies the competition between the necking process (brought about by the drop now having the same polarity as the homophase) and pumping process (due to surface tension) is similar to the case of a DC field, as the electric relaxation time is much faster than that of the mechanical pumping process. Therefore the drop sees the low frequency pulse electric field essentially the same as a DC field, hence promoting secondary droplets formation. So the results in the case of a low frequency are the same as that of the DC field regardless of the waveform type. In the presence of PEF the off-period mitigates necking and allows the process of drainage of the primary drop content into bulk homophase without being adversely affected by the electric field. As shown in Fig. 4, the sawtooth waveform is the most effective one, as the volume ratio (VR) follows:  $VR_{square} \geq VR_{sin} \geq VR_{sawtooth}$ . As the electrostatic force following the film rupture is mainly responsible for the necking process and hence responsible for the secondary droplets formation, the more effective electric field strength (meaning more on-time period and hence exposing the drop to this period) the stronger the necking process and subsequently the bigger the volume of secondary droplets detached from primary drop while coalescing. Therefore when the two latter waveforms are applied to the primary drop coalescing with the interface, the on-time part of

waveform prevails for a considerably shorter time than the square waveform, leading to weakening of the necking process against the pumping process. Also it is observed in Fig. 4 that the values of volume ratio under the action of these two waveforms approximately coincide since the difference between their on-time periods is negligible. At high frequencies the on-time period for the three waveforms comes close, hence the volume of the secondary droplets formed reaches a unique value which is close to zero. This is a desirable trend as it suppresses the secondary droplets formation. Hence an increase in the field frequency is useful up to a certain value, beyond which further increase is not effective anymore.

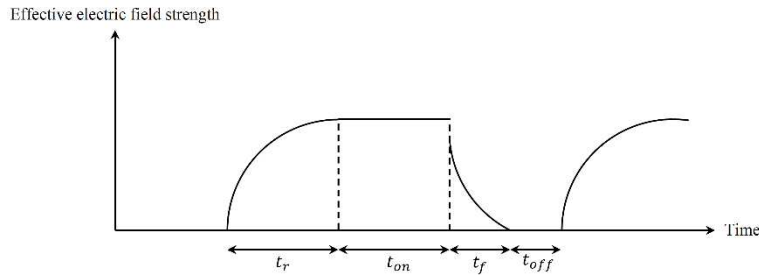


Fig. 5. A schematic typical waveform with four time periods including  $t_r$ ,  $t_{on}$ ,  $t_f$  and  $t_{off}$ .

### 3.2. Drop-Drop Coalescence

To show the effect of PEF on reducing and suppressing the secondary droplets formation some qualitative observations on the behaviour of coalescing drop pairs subjected to an electric field are first presented. Three distinct coalescence patterns are distinguishable in drop-drop coalescence at low frequency PEF and DC electric field: complete coalescence, partial coalescence and non-coalescence. Figure 6 shows a complete coalescence pattern ([Supplementary movie #2](#)). In this case the upper drop approaches the stationary lower drop sitting on the insulated bottom electrode due to gravity and mostly electrostatic forces. The local electric field strength in the gap between the drop surfaces increases rapidly, causing some drop elongation, followed by the rupture of the oil film and formation of neck. At this stage the surface tension merges the two drops completely. This pattern is ideal as it leads to a bigger resultant drop without producing any secondary droplets.

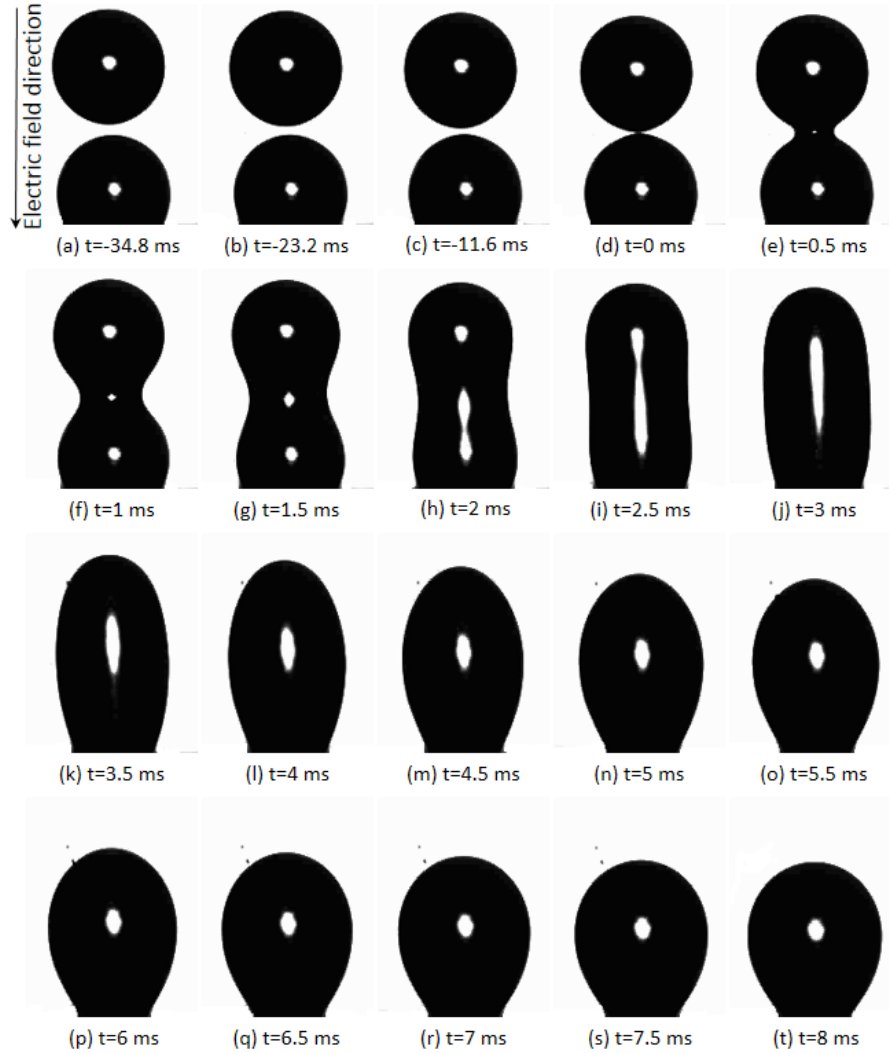


Fig. 6. Time sequence of a complete coalescence pattern for drop pair of  $829 \pm 1 \mu\text{m}$  diameter under very low frequency PEF or DC electric field strength of 150 V/mm

In contrast when a typical partial coalescence takes place the two primary drops do not merge entirely and the electric field pulls the coalescing drops apart producing secondary droplets by necking, generally one main droplet and a number of much finer ones. In fact this process produces several coalescence patterns, ranging from weak partial coalescence (WPC) to strong partial coalescence (SPC), as shown in Figs 7 and 8 ([Supplementary movies #3 and #4](#)). For the former the volume of secondary droplets produced is low and this in turn reduces the probability of their disintegration into further fine droplets as a result of the electric field stress. In the latter case the produced secondary droplets volume is comparable with the volume of any of the two primary drops. In this case the large secondary droplets experience high electric field strengths and could break into much finer droplets, as shown in Fig. 8. This is obviously very undesirable in terms of emulsion separation performance.

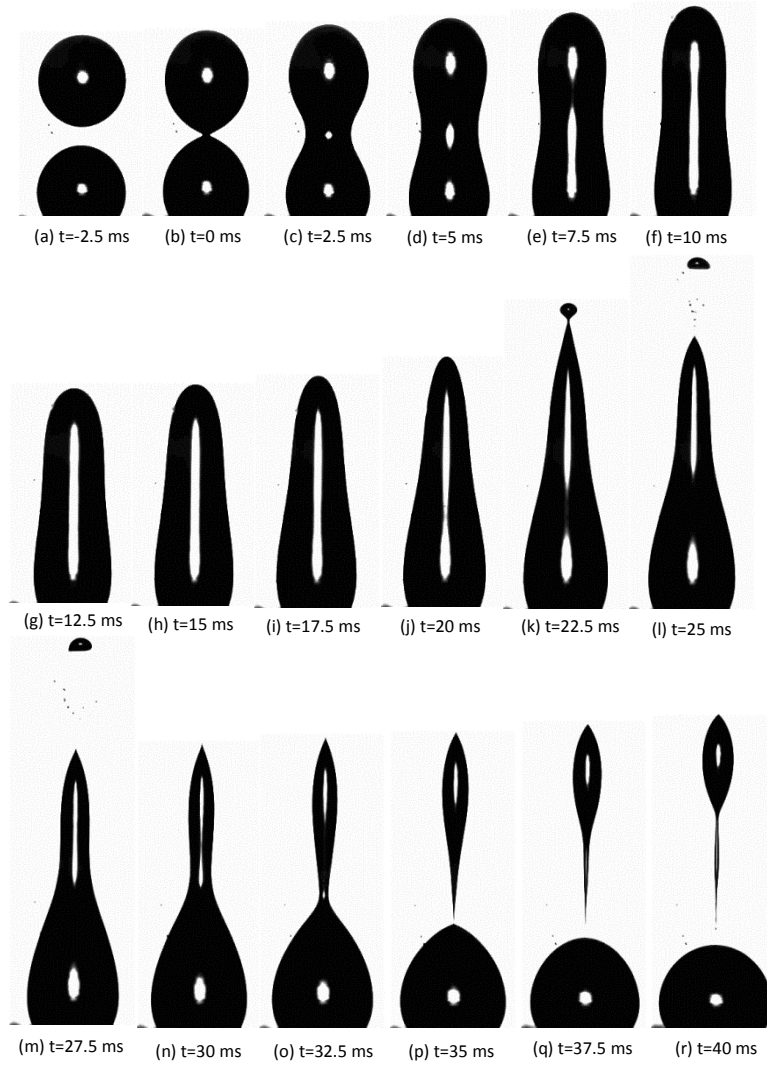


Fig. 7. Time sequence of a typical weak partial coalescence (WPC) pattern for drop pair of  $1196 \pm 4 \mu\text{m}$  diameter under very low frequency PEF or DC electric field strength of  $450 \text{ V/mm}$

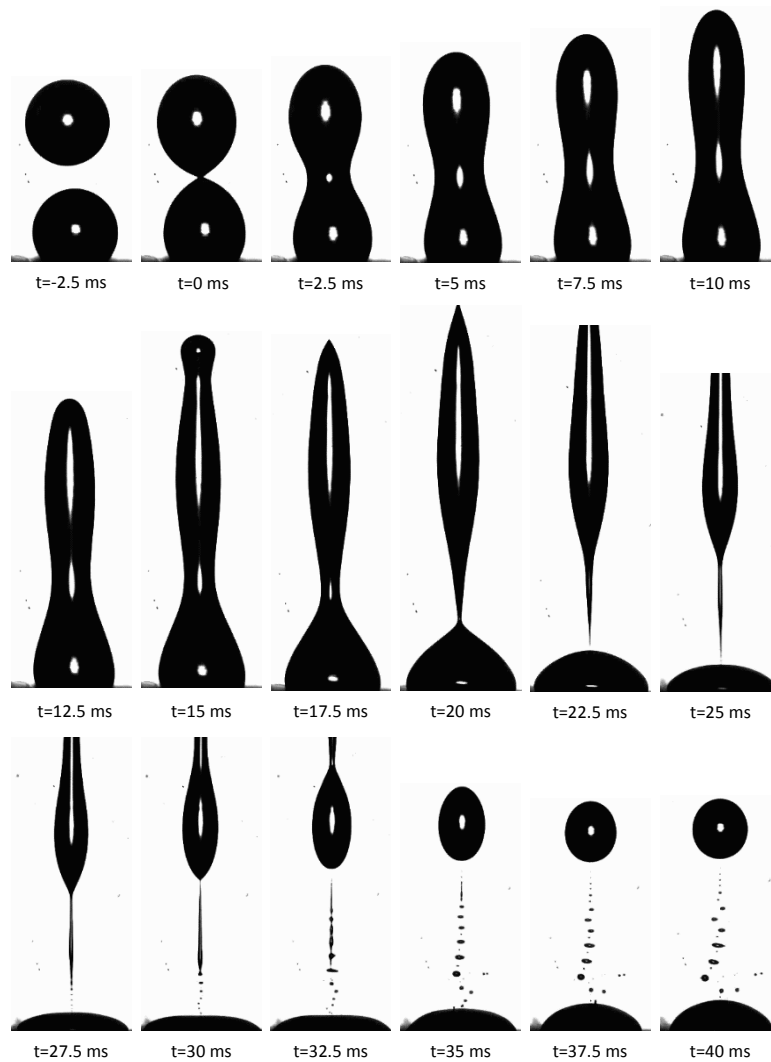


Fig. 8. Time sequence of a typical strong partial coalescence (SPC) pattern for drp pair of  $1196 \pm 4 \mu\text{m}$  diameter under very low frequency PEF or DC electric field strength of 551 V/mm

A non-coalescence pattern is shown in Fig. 9. This pattern is observed under various conditions, such as in the presence of surfactants, affecting the interfacial tension. The surfactant presence also affects the partial coalescence quality. For example for a given electric field strength and sizes of a drop pair, the WPC may change into SPC because of the surfactant presence. As natural surfactants are usually present in water-in-oil emulsions, therefore, it is of crucial importance to control and manipulate the effect of their presence in emulsions. To examine the effect of interfacial tension on appearance of various patterns of coalescence, an anionic surfactant SDS with concentration of 1 g/l was used which is soluble in the dispersed water phase. When a water drop pair of  $829 \pm 1 \mu\text{m}$  diameter containing SDS is subjected to the electric field strength range from 150 V/mm to 551 V/mm several different behaviours are observed as described below. For a drop pair subjected to 150 V/mm electric field strength, a

complete coalescence pattern is observed, whilst under a higher electric field strength (higher than 250 V/mm) a non-coalescence pattern prevails as illustrated in Fig. 9.

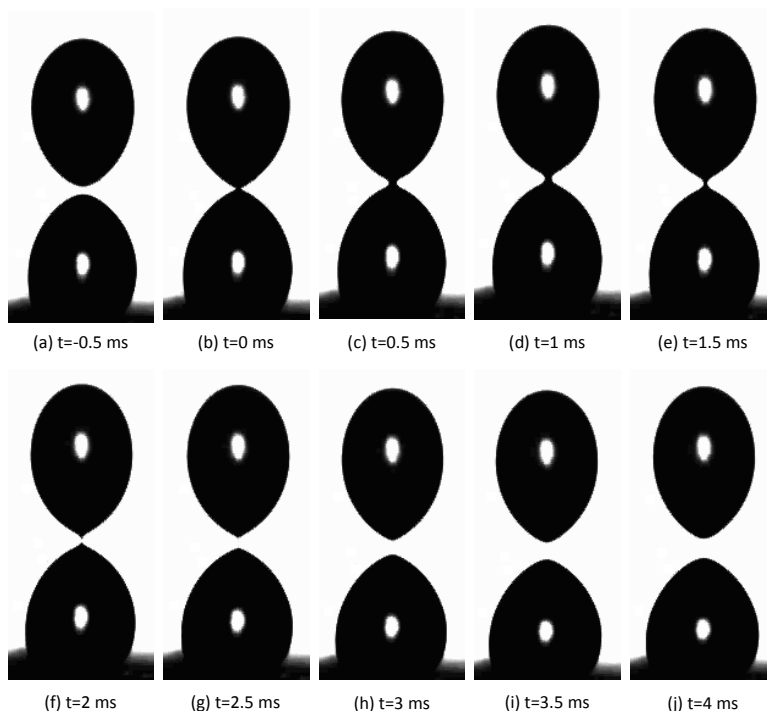


Fig. 9. Time sequence of a typical non-coalescence pattern occurrence for a drop pair of  $829 \pm 1 \mu\text{m}$  diameter containing 1 g/l SDS under very low frequency PEF or DC electric field strength of 350 V/mm.

Here when the upper falling drop reaches a critical distance from the lower drop the local electric field in the gap between the two drops increases rapidly and a narrow bridge (Fig. 9 (b)) forms and connects the drops together. However, within a short period following rupture (about 1.5 ms) the bridge thickness reduces to  $9 \mu\text{m}$  (Fig. 9 (e)) and the drops are pulled apart. This behaviour is a result of the surface tension force inability to overcome the electrostatic force, as for the same size drop pair in the absence of surfactants a complete coalescence is observed. In the absence of an electric field, the non-polar tail of SDS surfactant covers the drops surfaces, especially in the area of approaching drop faces and prevents the two drops from direct contact which is necessary for coalescence [48]. In the presence of an electric field, as soon as an electrical contact is established the two drops experience charge transfer and polarisation, subjecting the drops to a pull off force, breaking the formed bridge after a very short time leading to a non-coalescence pattern. The SDS presence reduces the interfacial tension to 10 mN/m, which leads to less rigidity in comparison with a de-ionized drop pair. This weakens the surface tension force in competing with the electrostatic force (Supplementary movie #5). Finally as shown in Fig. 10 for higher strengths from 350 V/mm to 551 V/mm, drops after a very fast contact (Fig. 10 (b)) are pulled apart from each other and the upper drop bounces and move up towards the positive electrode. The feature formed in Fig. 10 (d) is interesting and requires an analysis to find out what processes give rise to to this strange shape. Finally the drop rising up is stretched and breaks into fine droplets because of the electrostatic pressure (Supplementary

movie #6). As seen in this figure, this pattern is undesirable and if a considerable percentage of drop-drop coalescences occur like this the separation performance will be adversely affected.

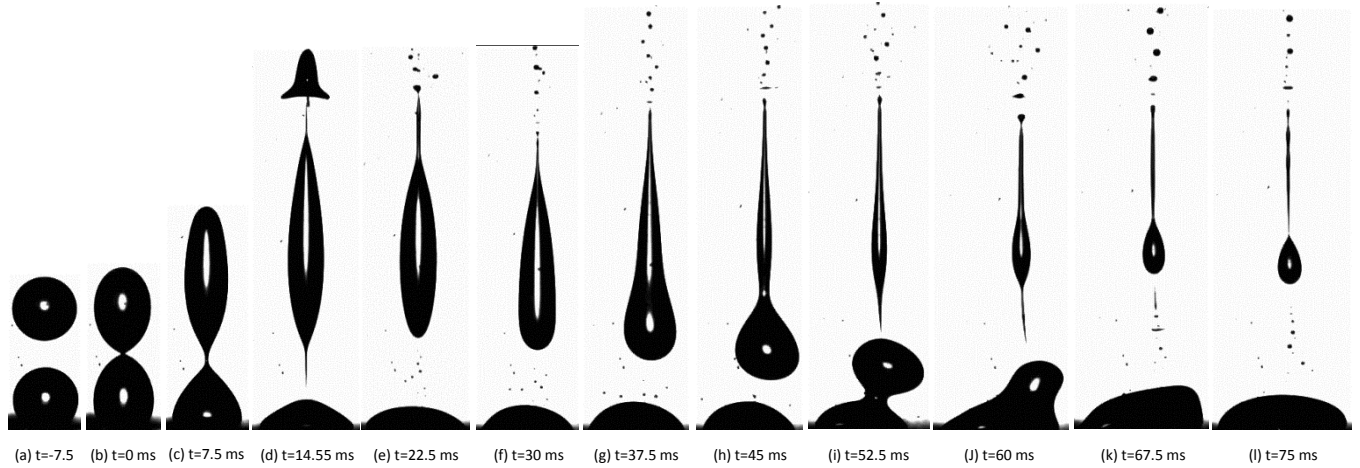


Fig. 10. Time sequence of a coalescence pattern of a drop pair of  $829 \pm 1 \mu\text{m}$  diameter containing 1 g/l SDS under very low frequency PEF or DC electric field strength of 551 V/mm.

To show the effect of PEF on drop-drop coalescence patterns, the application of PEF to a drop pair with diameter of  $1196 \pm 4 \mu\text{m}$  is considered under an electric field of 651 V/mm in amplitude and different frequencies between 0 (a DC field) to 200 Hz. The selection of such a relatively large drop pair and field amplitude was intentionally made to produce conditions conducive to secondary droplets formation, as in the case of SPC occurring under low frequency PEF of 551 V/mm in Fig. 8. By increasing the frequency up to 50 Hz, coalescence of drops follows a partial coalescence pattern, beginning with a strong partial coalescence at low frequencies and gradually ending up with a weak partial coalescence at 50 Hz. The quality of drop pair coalescence at 50 Hz is shown in Fig. 11.

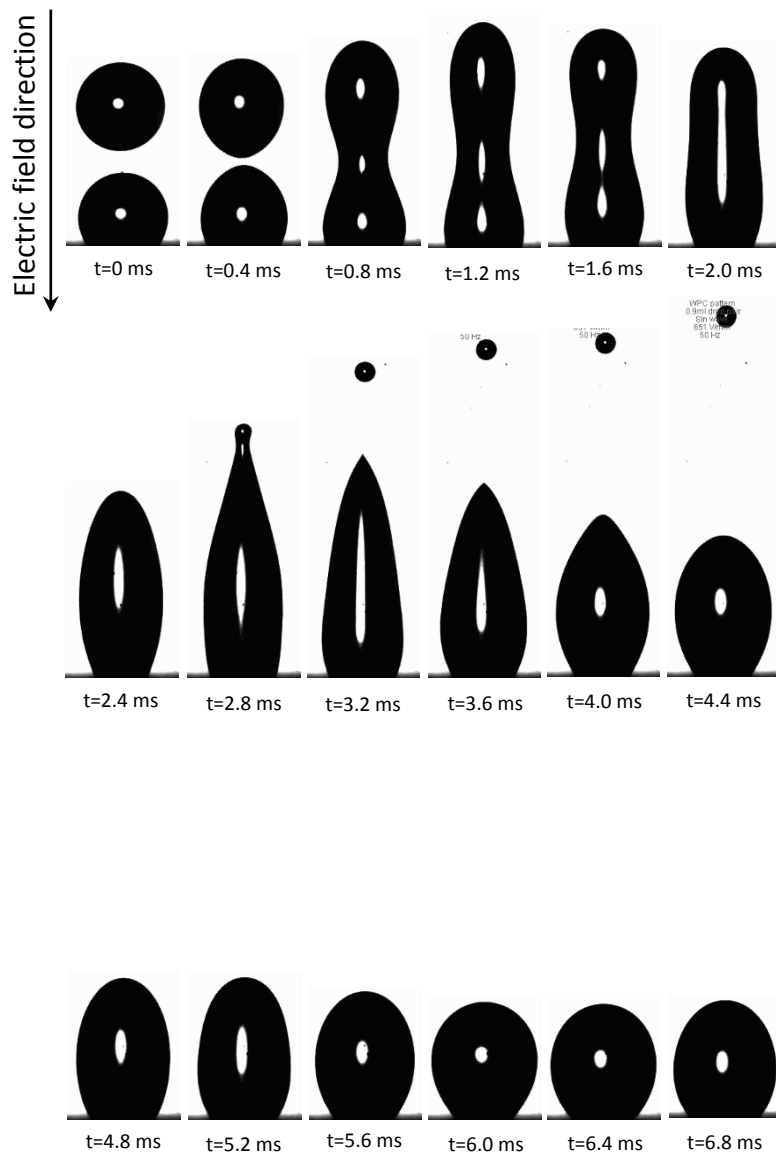


Fig. 11. Coalescence of a drop pair with a diameter of  $1196 \pm 4 \mu\text{m}$  under a sinusoidal waveform pulsed electric field with amplitude of  $651 \text{ V/mm}$  and pulse frequency of  $50 \text{ Hz}$ .

On further increasing the frequency beyond  $50 \text{ Hz}$  as shown in Fig. 12 the coalescence pattern switches from WPC to an ideal (complete) coalescence pattern ([Supplementary movie #7](#)). The experiments were repeated at frequencies higher than  $100 \text{ Hz}$  and observations of the video records suggests that the threshold frequency that shifts a non-ideal coalescence pattern

(WPC and SPC) to an ideal one is dependent on the PEF amplitude and size of primary drop pairs. For bigger primary drop pairs and larger amplitudes of PEF the threshold frequency would be higher. Beyond the threshold frequency, as it can be seen in the Fig. 12, the drop pair while oscillating finally merge and do not leave any secondary droplets behind. Therefore using PEF at higher than a threshold frequency clearly acts synergistically with the surface tension forces (helping pumping process) and against the electrostatic force (helping the necking process, as it attempts to detach drop/droplets and creating a highly unfavorable SPC pattern).

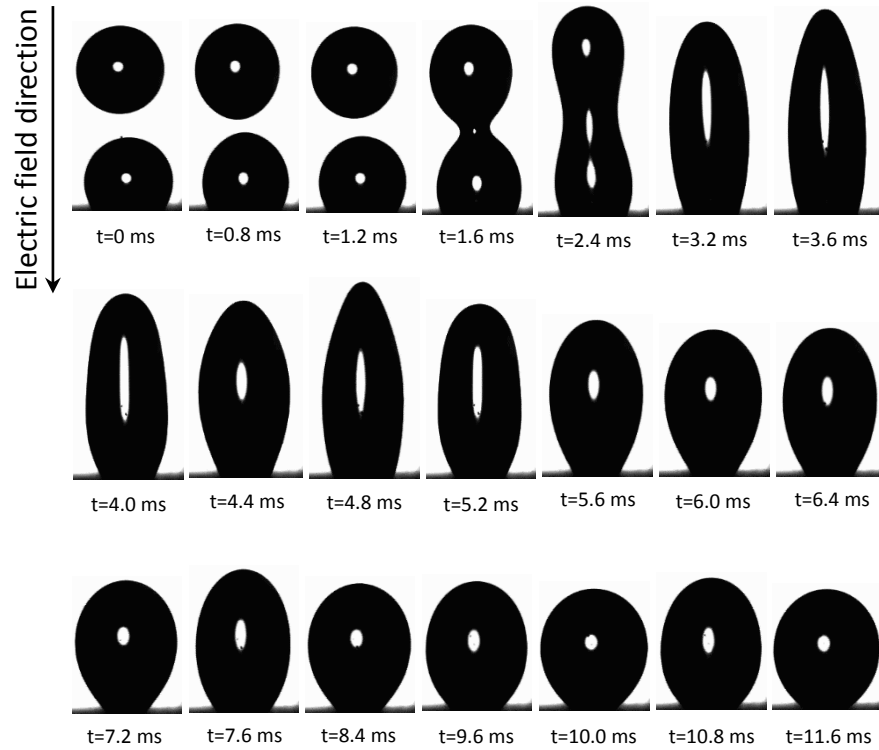


Fig. 12. Coalescence of a drop pair with a diameter of  $1196 \pm 4 \mu\text{m}$  under a sinusoidal waveform pulsed electric field amplitude of  $651 \text{ V/mm}$  and pulse frequency of  $100 \text{ Hz}$ .

The use of pulsatile electric fields is clearly advantageous, as it provides potential to apply higher electric field strengths in comparison with a DC field without concerns about the unfavorable secondary droplets formation.

#### 4. Conclusions

The effect of three different waveforms of a pulsatile electric field, i.e. square, sinusoidal and sawtooth, on the coalescence process of an aqueous droplet with a planar aqueous interface as well as of a drop pair was investigated. It is shown that the secondary droplets produced at very low frequency PEF or a DC electric field may be suppressed by increasing the frequency of PEF. By normalizing the total volume of the secondary droplets formed with respect to the initial drop volume, it is quantitatively shown that the sawtooth waveform is the most efficient shape to reduce the secondary droplets formation. High speed video observations suggest that the electric field strength falling to zero as rapidly as possible, once a connection is made between the two

coalescing entities, is helpful in mitigating the formation of secondary droplets. For the three waveforms examined, by increasing the frequency there is a threshold frequency above which a non-ideal patterns (WPC and SPC) shifts to an ideal pattern, depending on the PEF amplitude and the size of primary drop pairs. For bigger primary drop pairs and larger amplitudes of PEF the threshold frequency would be higher. Above the threshold frequency the drop pairs oscillate and finally merge without leaving any secondary droplets behind. The volume ratio of the secondary droplets approaches an asymptotic value very close to zero. This is an ideal pattern for the drop-interface and drop pair coalescence in water-in-oil emulsions, as it leads to improving the emulsion separation performance.

## Acknowledgements

This work could not be done without generous help from a number of people at the University of Leeds. Thanks are especially due to Drs Ali Hassanpour, Massih Pasha, Javad Khangostar, Graham Calvert, Colin Hare, Nejat Rahmanian, and Messrs Robert Harris, and Tarsem Hunjan. The authors are also grateful for the helpful comments of Dr Vincenzino Vivacqua and Mr Sameer Mhatre.

## References:

1. J. Sjöblom, E.E. Johnsen, A. Westvik, M.H. Ese, J. Djuve, I.H. Auflem, et al. (2001) In *Encyclopedic Handbook of Emulsion Technology*, edited by J. Sjöblom; New York: Marcel Dekker.
2. S.E. Friberg, S.J., *Emulsions*, in: *Kirk-Othmer Encyclopedia of Chem. Technol.*, 4th ed., Vol. 9, 1996, and p. 393-413.
3. J.S. Eow and M. Ghadiri, *Electrostatic enhancement of coalescence of water droplets in oil: a review of the technology*. *Chemical Engineering Journal*, 2002. **85**(2–3): p. 357-368.
4. F.B.-W. Pierre-Gilles de Gennes, *David Quere Capillarity and Wetting Phenomena: Drops, Bubbles, Pearls, Waves*. 2004, New York: Springer.
5. T. Frising, C. Noïk and C. Dalmazzone, *The Liquid/Liquid Sedimentation Process: From Droplet Coalescence to Technologically Enhanced Water/Oil Emulsion Gravity Separators: A Review*. *Journal of Dispersion Science and Technology*, 2006. **27**(7): p. 1035-1057.
6. S. Kokal, *Crude Oil Emulsions: A State-Of-The-Art Review*. *SPE Production & Facilities*, 2005. **20**: p. 5-13.
7. J. Sjöblom, N. Aske, I. Harald Auflem, Ø. Brandal, T. Erik Havre, Ø. Sæther, A. Westvik, E. Eng Johnsen and H. Kallevik, *Our current understanding of water-in-crude oil emulsions.: Recent characterization techniques and high pressure performance*. *Advances in Colloid and Interface Science*, 2003. **100–102**(0): p. 399-473.
8. C.P. Whitby, D. Fornasiero and J. Ralston, *Effect of oil soluble surfactant in emulsions stabilised by clay particles*. *Journal of Colloid and Interface Science*, 2008. **323**(2): p. 410-419.
9. M.H. Ese, X. Yang and J. Sjöblom, *Film forming properties of asphaltenes and resins. A comparative Langmuir–Blodgett study of crude oils from North Sea, European continent and Venezuela*. *Colloid and Polymer Science*, 1998. **276**(9): p. 800-809.
10. I. Kralova, J. Sjöblom, G. Øye, S. Simon, B.A. Grimes and K. Paso, *Heavy Crude Oils/Particle Stabilized Emulsions*. *Advances in Colloid and Interface Science*, 2011. **169**(2): p. 106-127.
11. J.D. McLean and P.K. Kilpatrick, *Effects of Asphaltene Solvency on Stability of Water-in-Crude-Oil Emulsions*. *Journal of Colloid and Interface Science*, 1997. **189**(2): p. 242-253.
12. K.J. Lissant, D.i.a., in: *Surfactant Science Series 13*, Marcel Dekker, New York, 1983.
13. R.A. Mohammed, A.I. Bailey, P.F. Luckham and S.E. Taylor, *Dewatering of crude oil emulsions 3. Emulsion resolution by chemical means*. *Colloids and Surfaces A: Physicochemical and Engineering Aspects*, 1994. **83**(3): p. 261-271.

14. J. Wu, Y. Xu, T. Dabros and H. Hamza, Effect of Demulsifier Properties on Destabilization of Water-in-Oil Emulsion. *Energy & Fuels*, 2003. **17**(6): p. 1554-1559.
15. V.B. Menon, i.P.B.E., *Encyclopedia of Emulsion Technology*, vol. 2, Marcel Dekker, Inc., 1985.
16. S. Dezhi, J. Shik Chung, D. Xiaodong and Z. Ding, Demulsification of water-in-oil emulsion by wetting coalescence materials in stirred- and packed-columns. *Colloids and Surfaces A: Physicochemical and Engineering Aspects*, 1999. **150**(1-3): p. 69-75.
17. R.A. Mohammed, A.I. Bailey, P.F. Luckham and S.E. Taylor, Dewatering of crude oil emulsions 1. Rheological behaviour of the crude oil–water interface. *Colloids and Surfaces A: Physicochemical and Engineering Aspects*, 1993. **80**(2-3): p. 223-235.
18. M. Goto, J. Irie, K. Kondo and F. Nakashio, Electrical demulsification of W/O emulsion by continuous tubular coalescer. *JOURNAL OF CHEMICAL ENGINEERING OF JAPAN*, 1989. **22**(4): p. 401-406.
19. C. Lesaint, W.R. Glomm, L.E. Lundgaard and J. Sjöblom, Dehydration efficiency of AC electrical fields on water-in-model-oil emulsions. *Colloids and Surfaces A: Physicochemical and Engineering Aspects*, 2009. **352**(1-3): p. 63-69.
20. S. Less, A. Hannisdal, E. Bjørklund and J. Sjöblom, Electrostatic destabilization of water-in-crude oil emulsions: Application to a real case and evaluation of the Aibel VIEC technology. *Fuel*, 2008. **87**(12): p. 2572-2581.
21. Christine Noik, Jiaqing Chen and C. Dalmazzone, Electrostatic Demulsification on Crude Oil: A State-of-the-Art Review, in *SPE International Oil & Gas Conference and Exhibition*. 2006, Society of Petroleum Engineers: Beijing, China.
22. J.S. Eow and M. Ghadiri, Drop–drop coalescence in an electric field: the effects of applied electric field and electrode geometry. *Colloids and Surfaces A: Physicochemical and Engineering Aspects*, 2003. **219**(1-3): p. 253-279.
23. J.S. Eow, M. Ghadiri, A.O. Sharif and T.J. Williams, Electrostatic enhancement of coalescence of water droplets in oil: a review of the current understanding. *Chemical Engineering Journal*, 2001. **84**(3): p. 173-192.
24. S. Less and R. Vilagines, The electrocoalescers' technology: Advances, strengths and limitations for crude oil separation. *Journal of Petroleum Science and Engineering*, 2012. **81**(0): p. 57-63.
25. O. Urdahl, K. Nordstad, P. Berry, N. Wayth, T. Williams, A. Bailey and M. Thew, Development of a New, Compact Electrostatic Coalescer Concept. *SPE Production & Facilities*, 2001. **16**: p. 4-8.
26. F.G. Cottrell, Process for separating and collecting particles of one liquid suspended in another liquid, US Patent 987114 (1911).
27. F.G. Cottrell, J.B. Speed, Separating and collecting particles of one liquid suspended in another liquid, US Patent 987,115 (1911).
28. H. Førde, Y. Schildberg, J. Sjöblom and J.-L. Volle, Crude oil emulsions in high electric fields as studied by dielectric spectroscopy. Influence of interaction between commercial and indigenous surfactants. *Colloids and Surfaces A: Physicochemical and Engineering Aspects*, 1996. **106**(1): p. 33-47.
29. P. Atten, Electrocoalescence of water droplets in an insulating liquid. *Journal of Electrostatics*, 1993. **30**(0): p. 259-269.
30. P.J. Bailes, J.G.M. Lee and A.R. Parsons, An Experimental Investigation into the Motion of a Single Drop in a Pulsed DC Electric Field. *Chemical Engineering Research and Design*, 2000. **78**(3): p. 499-505.
31. G.E. Charles and S.G. Mason, The coalescence of liquid drops with flat liquid/liquid interfaces. *Journal of Colloid Science*, 1960. **15**(3): p. 236-267.
32. J.S. Eow and M. Ghadiri, The behaviour of a liquid–liquid interface and drop-interface coalescence under the influence of an electric field. *Colloids and Surfaces A: Physicochemical and Engineering Aspects*, 2003. **215**(1-3): p. 101-123.
33. M. Mousavichoubeh, M. Ghadiri and M. Shariaty-Niassar, Electro-coalescence of an aqueous droplet at an oil–water interface. *Chemical Engineering and Processing: Process Intensification*, 2011. **50**(3): p. 338-344.
34. M. Mousavichoubeh, M. Shariaty-Niassar and M. Ghadiri, The effect of interfacial tension on secondary drop formation in electro-coalescence of water droplets in oil. *Chemical Engineering Science*, 2011. **66**(21): p. 5330-5337.
35. S.E. Taylor, Investigations into the electrical and coalescence behaviour of water-in-crude oil emulsions in high voltage gradients. *Colloids and Surfaces*, 1988. **29**(1): p. 29-51.

36. T.J. Williams and A.G. Bailey, Changes in the Size Distribution of a Water-in-Oil Emulsion Due to Electric Field Induced Coalescence. *Industry Applications, IEEE Transactions on*, 1986. **IA-22**(3): p. 536-541.
37. P.J. Bailes, Resolution of emulsions, US Patent 5 580 464 (1996).
38. S.E. Taylor, Theory and practice of electrically enhanced phase separation of water-in-oil emulsions. *Trans. IChemE*, 1996. **74**(A): p. 526–540.
39. J. Drelich, G. Bryll, J. Kapczynski, J. Hupka, J.D. Miller and F.V. Hanson, The effect of electric field pulsation frequency on breaking water-in-oil emulsions. *Fuel Processing Technology*, 1992. **31**(2): p. 105-113.
40. S. Less, A. Hannisdal and J. Sjöblom, Dehydration Efficiency of Water-in-Crude Oil Emulsions in Alternating Current Electrical Fields. *Journal of Dispersion Science and Technology*, 2010. **31**(3): p. 265-272.
41. P.J. Bailes, Larkai, S.K.L., An experimental investigation into the use of high voltage d.c. fields for liquid phase separation. *Trans. IChemE*, 1981. **59**(4): p. 229–237.
42. P.J. Bailes, Larkai, S.K.L., Liquid phase separation in pulsed d.c. fields. *Trans. IChemE*, 1982. **60**(2): p. 115–121.
43. P.J. Bailes and P.D. Dowling, The production of pulsed E.H.T. voltages for electrostatic coalescence. *Journal of Electrostatics*, 1985. **17**(3): p. 321-328.
44. Y. Zhang, Y. Liu and R. Ji, Dehydration efficiency of high-frequency pulsed DC electrical fields on water-in-oil emulsion. *Colloids and Surfaces A: Physicochemical and Engineering Aspects*, 2011. **373**(1–3): p. 130-137.
45. Y. Zhang, Y. Liu, R. Ji, F. Wang, B. Cai and H. Li, Application of variable frequency technique on electrical dehydration of water-in-oil emulsion. *Colloids and Surfaces A: Physicochemical and Engineering Aspects*, 2011. **386**(1–3): p. 185-190.
46. O.-M. Midtgård, Electrostatic field theory and circuit analysis in the design of coalescers with pulsed dc voltage. *Chemical Engineering Journal*, 2009. **151**(1–3): p. 168-175.
47. B.S. Hamlin, J.C. Creasey and W.D. Ristenpart, Electrically Tunable Partial Coalescence of Oppositely Charged Drops. *Phys. Rev. Lett.*, 2012. **109**(9): p. 094501-094505.
48. K. Giribabu and P. Ghosh, Adsorption of nonionic surfactants at fluid–fluid interfaces: Importance in the coalescence of bubbles and drops. *Chemical Engineering Science*, 2007. **62**(11): p. 3057-3067.